Organic Electronics 15 (2014) 582–589

Contents lists available at ScienceDirect

Organic Electronics

journal homepage: www.elsevier.com/locate/orgel

Star-shaped self-assembly of an organic thin film transistor sensor in the presence of Cu^{2+} and CN^- ions

Mohan Ramesh [b], Yuan-Ruei You [c], Muthaiah Shellaiah [b], Meng-Chyi Wu [c], Hong-Cheu Lin [b,*], Chih-Wei Chu [a,d,*]

[a] Research Center for Applied Sciences, Academia Sinica, Taipei 115, Taiwan, ROC
[b] Department of Materials Science and Engineering, National Chiao Tung University, Hsinchu 300, Taiwan, ROC
[c] Institute of Electronics Engineering, National Tsing Hua University, Hsinchu 300, Taiwan, ROC
[d] Department of Photonics, National Chiao Tung University, Hsinchu 300, Taiwan, ROC

ARTICLE INFO

Article history:
Received 23 August 2013
Received in revised form 26 November 2013
Accepted 7 December 2013
Available online 17 December 2013

Keywords:
Pyrene
Thin film transistor
Metal ion
Cyanide anion
Self-assembly
Sensor

ABSTRACT

In this study we developed organic thin film transistors (OTFTs) for the sensing of metal ions and anions through the self-assembly of a pentacene/Schiff base pyrene derivative. Our bilayer OTFTs displayed attractive device parameters: an electron mobility (μ) of 0.12 $cm^2 V^{-1} s^{-1}$, a threshold voltage (V_{th}) of 22.20 V, and a five-orders-of-magnitude on/off ratio. This device was sensitive toward Cu^{2+} among 13 metal cations and toward CN^- among nine anions, as measured through changes in the values of V_{th} and I_{off} in the presence of Cu^{2+} cations and a change in the value of I_{sat} in the presence of CN^- anions. We observed selectivity toward both of these ions in mixed ion solutions, with sensitivity over different concentrations (from 20 to 350 μM for Cu^{2+}; from 100 to 350 μM for CN^-) as well as in sea water. The pyrene derivative self-assembled through pyrene–pyrene* coordination in the presence of Cu^{2+} ions; the rods of the pyrene derivative broke into smaller pieces upon formation of benzoxazole rings in the presence of CN^- ions, as confirmed using atomic force microscopy and fourier transform attenuated total reflection spectroscopy.

1. Introduction

The detection of heavy metals and anions in the environment is necessary because of increasing threats from pollution. To identify these ions, ideally we would replace optical sensors, which function based on changes in color and/or fluorescence intensity (or emission wavelength), with devices that are more inexpensive, portable (handheld), lighter in weight, and user-friendly; organic thin film transistors (OTFTs) appear to be one such tool [1]. Although OTFTs find widespread use in flexible high-resolution display technologies, very little research has been performed into their applicability in sensor technologies (mainly pressure, vapor, liquid, near infrared, dopamine and some biological sensors) [2]. To improve their utility as sensors, we develop OTFTs for the detection of metal ions and anions.

Among the metal ions, copper(II) (Cu^{2+}) is third most abundant essential trace element for the human body, performing important roles in many physiological processes [3]. Increasing the level of Cu^{2+} can affect the organs (e.g., the liver and kidneys) and block various enzymes that are responsible for essential biochemical processes in the human body. Copper-containing waste water can arise from coal mining (and metal manufacturing industries), electroplating processes, and the corrosion of pipes [4]. Among all anions, the detection of cyanide (CN^-) is the most important because of its extreme toxicity, which arises from its binding to cytochromes and its inhibition of electron transport chain in mitochondria [5]; in

* Corresponding authors. Address: Research Center for Applied Sciences, Academia Sinica, Taipei 115, Taiwan, ROC. Tel.: +886 2 27898000x70; fax: +886 2 27826680 (C.-W. Chu). Tel.: +886 3 5712121x55305; fax: +886 3 5724727 (H.-C. Lin).
E-mail addresses: linhc@cc.nctu.edu.tw (H.-C. Lin), gchu@gate.sinica.edu.tw (C.-W. Chu).

1566-1199/$ - see front matter © 2013 Elsevier B.V. All rights reserved.
http://dx.doi.org/10.1016/j.orgel.2013.12.007

addition, it can lead directly to the death of human beings as well as aquatic animals, at low concentrations by depressing the central nervous system. Because CN^- is used widely in the extraction of gold and silver, tanning, steel manufacturing, metal electroplating, the manufacture of nitrile, nylon, and acrylic plastics, and in the petrochemical and photographic industries [6], it is also found extensively in waste water. Accordingly, there is high demand for the development for rapid, sensitive, and selective means of detection of both Cu^{2+} and CN^- ions. At present, their detection and characterization are best performed using colorimetric and/or fluorescent chemosensors [7], which require expensive and sophisticated instruments, prolong detection times, and skilled operators. To overcome these limitations, we are interested in developing three-terminal device OTFTs for use as sensors of these ions.

OTFTs have several attractive features: they are inexpensive to produce, they can be formed over large areas with mechanical flexibility, they consume lower amounts of power, and their analysis times are faster relative to those of optical detection systems. Not all OTFTs can be used to fabricate sensors; those that can feature (I) functionalized single active layers or an electrolyte gate [8], (II) incorporate nanoparticles in the work area [9], or (III) possess a bilayer (semiconductor/ligand) device structure [10]. The devices of types I and II can be complicated to prepare; for example, the functionalized active layer might not be stable in aqueous media or the incorporated nanoparticles might increase the resistance of the device. To avoid these difficulties, in this study we chose to prepare bilayer devices (semiconductor/ligand) for the detection of Cu^{2+} and CN^- ions. Here, we employed pentacene as the semiconductor layer and a Schiff base-type pyrene derivative (P) as the second layer for the probe. Pentacene is a well-established semiconductor that is used widely in many applications because it is stable in air and in aqueous media [11]. Over the past two decades, sensors based on self-assembled monolayers of pyrene derivatives have been constructed for the detection of a wide variety of targets, metal ions, anions [12], and dopamine [13]; it has also been used to great advantage in biological probes [14], OTFTs [15], and solar cells [16]. Furthermore, pyrene probes can self-assemble to form dimeric structures ($P–P^*$) upon the addition of ions [17].

In this study we developed pentacene/P-based OTFTs for the detection of both Cu^{2+} and CN^- ions, either alone or mixed with other ions, and at various concentrations in the range from 20 to 350 μM. We monitored the sensitivity of the sensor toward Cu^{2+} ions by observing the shift of the threshold voltage (V_{th}) and off current (I_{off}) at −60 V and toward CN^- ions by observing the change in the value of I_{sat} at −60 V. Our sensor could detect Cu^{2+} and CN^- ions at concentrations as low as 20 and 150 μM, respectively, as a result of self-assembly events that occurred upon adding Cu^{2+} and CN^- ions.

2. Materials and methods

2.1. Materials

Pentacene, poly(4-vinylpyridine) (PVP), poly(melamine-co-formaldehyde), $Mn(OAc)_2$, $MgSO_4$, all chloride salts (Fe^{2+}, Cu^{2+}, Ba^{2+}, Sn^{2+}, Ni^{2+}, Zn^{2+}, Ag^{2+}, Ca^{2+}, Co^{2+}, Cs^+, Al^{2+}), and all tetrabutylammonium salts (CN^-, PO_4^{3-}, I^-, HSO_4^-, F^-, NO_3^-, ClO_4^-, Cl^-, Br^-) were purchased from Sigma–Aldrich. The Schiff base pyrene derivative was synthesized following a literature procedure [18].

2.2. Device fabrication and characterization

OTFTs were obtained from highly doped n-type Si wafers (100) covered with silicon dioxide (SiO_2; thickness: 300 nm) as a gate dielectric (2 cm × 2 cm). After cleaning with detergent, acetone, and isopropyl alcohol, the wafer was treated in a UV-ozone cleaner for 30 min. The ozone-treated substrates were spin-coated with a solution of PVP (11 wt%) and poly(melamine-co-formaldehyde) (4 wt%) in PGMEA at 4000 rpm for 60 s. The substrate was then prebaked at 100 °C for 5 min, followed by baking at 200 °C for 20 min to crosslink the polymer. Pentacene (40 nm) was thermally evaporated (pressure: 5×10^{-6} torr) onto the C–PVP film; the Schiff base pyrene derivative was then thermally evaporated onto the pentacene layer under the same pressure. Following the preparation of the active layer, Au source and drain electrodes (thickness: 50 nm) were thermally evaporated through a shadow mask [channel width (W): 200 μm; channel length (L): 2000 μm; pressure: 5×10^{-6} torr]. The mobility was calculated by considering the dielectric constant of SiO_2 and the thickness of the C–PVP.

2.3. Device characterization and analyses

Fabricated devices were characterized using a Keithley 4200 semiconductor characterization system. Atomic force microscopy (AFM) images were recorded using a Bruker Dimension Icon atomic force microscope; Fourier transform attenuated total reflection (FT-ATR) spectra were recorded using a PerkinElmer spectrum 100 series spectrometer.

2.4. Sensor devices measurement

Solutions of the various metal cations and anions were prepared by dissolving salts in deionized water at concentrations of 10^{-3} M; solutions containing pairs of metal cations and anions were prepared by mixing solutions of the single metal ions of the same concentration (10^{-3} M) at a 1:1 ratio. The sensor devices were tested by placing a drop (1 μL) of a solution of the metal cation on top of the channel, drying for 60 min, and then measuring under an N_2 atmosphere. Solutions of Cu^{2+} and CN^- ions of various concentrations were prepared by diluting the stock solution (1 mM) to 20, 50, 150, 250, and 350 μM. The value of ΔV_{th} was calculated by subtracting the threshold voltage shift (V_{th}) in the presence of ions from that in the absence of ions. The difference in the values of I_{sat} was calculated in a similar manner.

3. Results and discussion

3.1. Pentacene/P device response

Fig. 1(a) displays the structure of the fabricated pentacene/P bilayer device. For the thermally evaporated semiconductor, dielectric surface roughness was an important factor toward obtaining a large carrier mobility, because molecular ordering of the grown pentacene film was controlled by the surface roughness of the gate dielectric. The surface roughnesses of both the dielectric materials (polymer and SiO_2) were virtually identical [19]. Because we wished to operate our devices in aqueous media, however, the result should not vary as much and the unmodified SiO_2/pentacene OTFT resulted in a positive value of V_{th} [19]. Therefore, we used a reserve polymer layer (C–PVP) to ensure the preparation of OTFTs that would exhibit stable operation and high electrical performance. We positioned the C–PVP film at the interface between the SiO_2 and the active layer. Fig. 1(b) presents the output characteristics of typical p-channel pentacene/P transistors operated at various gate voltages (V_G); Fig. 1(c) plots the values of I_{DS} with respect to the values of V_G at a constant value of V_{DS} of −60 V. The device parameters that we extracted from the bilayer were an electron mobility (μ) of 0.12 cm^2 - V^{-1} s^{-1}, a threshold voltage (V_{th}) of −22.20 V, and an on/off ratio extending over five orders of magnitude. Therefore, we employed this device platform to prepare a sensor for Cu^{2+} and CN^- ions.

3.2. Cu^{2+} ions sensitivity and selectivity studies in OTFTs

Several parameters can be measured to determine the sensitivity and selectivity of OTFT sensors, including changes in the values of V_{th}, I_{on}, I_{off}, and I_{sat}. To test the performance of our sensor for Cu^{2+} ions, we monitored the variations in V_{th} and I_{off} (Fig. 2(a) and (b)). To discern whether these changes were due to the Cu^{2+} ions or deionised water, we monitored the device in the presence of deionised water and noticed the negligible change in device performance (Fig. S1 (ESI)). To confirm the selectivity the device was measured in doubly charged (Fe^{2+}, Mg^{2+}, Mn^{2+}, Ba^{2+}, Sn^{2+}, Ni^{2+}, Zn^{2+}, Ag^{2+}, Ca^{2+}, Co^{2+}, Al^{2+}) and singly charged (Cs^+) ions (Fig. 2); the extracted values of ΔV_{th} for these cations ranged from 3 to 10 V while the off currents (A) ranged from 1×10^{-10} to 5×10^{-9}. For Cu^{2+} ions, the value of ΔV_{th} was approximately 25 V and the value of I_{off} was 1×10^{-7}; these significantly enhanced values resulted from the presence of the P units, which self-assembled to form P–P* species, with the disappearance of the OH group, upon adding the Cu^{2+} ions, as displayed in the insets to Fig. 2(a) and (c) [18]. The formation of P–P* complexes only in the presence of Cu^{2+} ions may have been due to the cavity size of the probe present in P matching the size of the Cu^{2+} ion, thereby leading to a large change in the value of ΔV_{th} and a decreases in the off current. None of the other ions (Fe^{2+}, Mg^{2+}, Mn^{2+}, Ba^{2+}, Sn^{2+}, Ni^{2+}, Zn^{2+}, Ag^{2+}, Ca^{2+}, Co^{2+}, Cs^+, Al^{2+}) matched the size of the probe cavity present in P and, therefore, did not facilitate the formation of P–P* complexes. Therefore, our pentacene/P

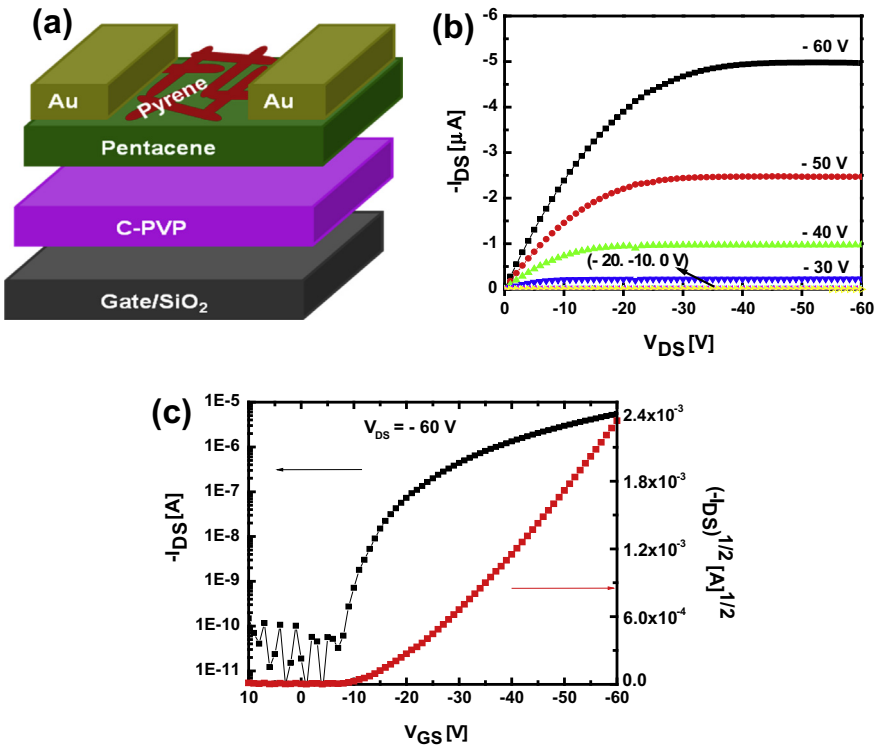

Fig. 1. (a) Structure of the device incorporating pentacene and the pyrene derivative. (b and c) Output and transfer characteristics of the p-channel OTFT containing pentacene and the pyrene derivative.

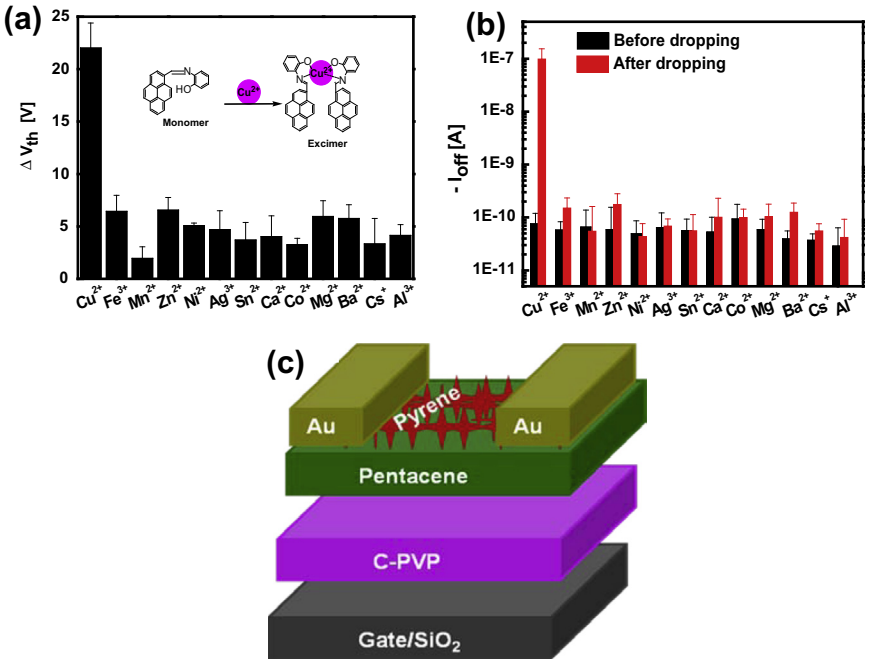

Fig. 2. (a) Differences in threshold voltage (ΔV_{th}) and (b) off current shifts (I_{off}) in the presence of various single metal ions. (c) Schematic representation of the self-assembly of star-shaped pyrene derivatives in the presence of Cu^{2+} ions.

transistors exhibited excellent sensitivity for Cu^{2+} ions among all of the tested single metal cations. Because an aqueous sample of environmental concern would probably not feature only a single type of metal ion, we extended our measurements of device performance to mixed-ion solutions in the presence and absence of Cu^{2+} ions (Fig. 3). When Cu^{2+} ions were present, the values of ΔV_{th} and I_{off} for the solutions containing the pair of mixed ions were similar to those of the Cu^{2+}-only solutions (from 20 to 27.5 V and from 5×10^{-7} to 3×10^{-6} A, respectively); in the absence of Cu^{2+} ions, however, the values of ΔV_{th} did not reach above 7 V and the values of I_{off} remained below 5×10^{-9} A (Fig. 3(a) and (b)).

Furthermore, to test the sensitivity of the device, we diluted a 1 mM stock solution of Cu^{2+} ions to different concentrations and then placed a drop of each solution on top of the different devices and attempted to measure the concentration. Fig. 3(c) reveals that upon increasing the concentration from 20 to 350 μM, the value of ΔV_{th} increased from 5 to 20 V and the value of I_{off} increased from 1×10^{-10} to 5×10^{-7} A. From these concentration data obtained with the single metal ion, we found that this device could detect Cu^{2+} ions at concentrations as low as 50 μM. To test this performance, we employed our sensor device to detect Cu^{2+} ions in a real sample in real time. When we employed our pentacene/P transistors to analyze sea water samples containing and free of Cu^{2+} ions, we observed the excellent changes in Cu^{2+} containing sea water at a concentration of 50 μM (Fig. S2 (ESI)).

3.3. Sensing mechanisms of Cu^{2+} ions

We used AFM (scale: 20 × 20 μm) and FT-ATR spectroscopy to examined the sensing mechanism of our device (see Fig. 4 and Fig. S3 (ESI)). The thermally evaporated P grew to form non-uniform thick rods, which broke into several pieces and self-assembled into star shapes upon the addition of Cu^{2+} ions (Fig. S3 (ESI) and Fig. 4(a)). Deprotonation of the OH moieties of the P units led to the formation of P–P* complexes through coordination with Cu^{2+} ions [18], causing the rods to self-assemble into a star shape. The FT-ATR spectra confirmed the disappearance of the signal for the OH groups of P at 3250–3500 cm^{-1} and the aliphatic region become broader near 3000 cm^{-1} after the addition of the Cu^{2+} ions (cf. Fig. 4(d) and (e)). The semiconductor property of P decreases with increasing the conductor behavior after forming P–P* complexes with Cu^{2+} ions [20]. The P–P* complexes were densely spread all over the channel (Fig. 4(a)) and decrease the channel resistance with increasing the pentacene carrier density. The high I_{off} current performance may be attributed to the presence of high carrier density in the channel. This ability to self-assemble in the presence of Cu^{2+} ions changed the values of V_{th} and I_{off} to greater degrees than those in the presence of the other metal ions. To further confirm the mechanism, we prepared monolayer devices containing only pentacene and used the cations (Cu^{2+}, Ca^{2+}, Zn^{2+}) to monitor the electrical behavior and we observed only negligible changes in the device performance (see Fig. S4 (ESI)). From this result it confirmed that the change in V_{th} and I_{off} was only due to P rods.

Using AFM, we affirmed the self-assembly processes occurring in both the presence and absence of Cu^{2+} in solutions containing mixed metal ions (cf. Fig. 4(b) and (c)). The AFM image of the sample obtained in the presence of mixed Cu^{2+} and Co^{2+} ions was similar to that obtained for the sample exposed to Cu^{2+} ions alone (Fig. 4(a)); in the absence of Cu^{2+} ions, the AFM image was similar to that in

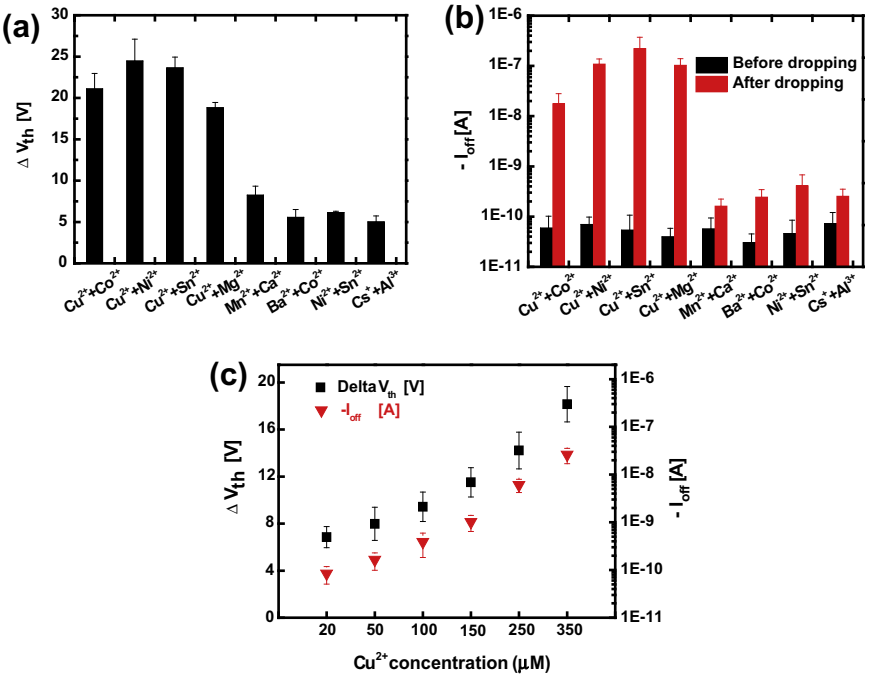

Fig. 3. (a) Differences in threshold voltage (ΔV_{th}) and (b) off current shifts (I_{off}) in the presence of pairs of different metal ions. (c) Differences in threshold voltage (ΔV_{th}) and off current shifts (I_{off}) in the presence of Cu^{2+} ions at various concentrations.

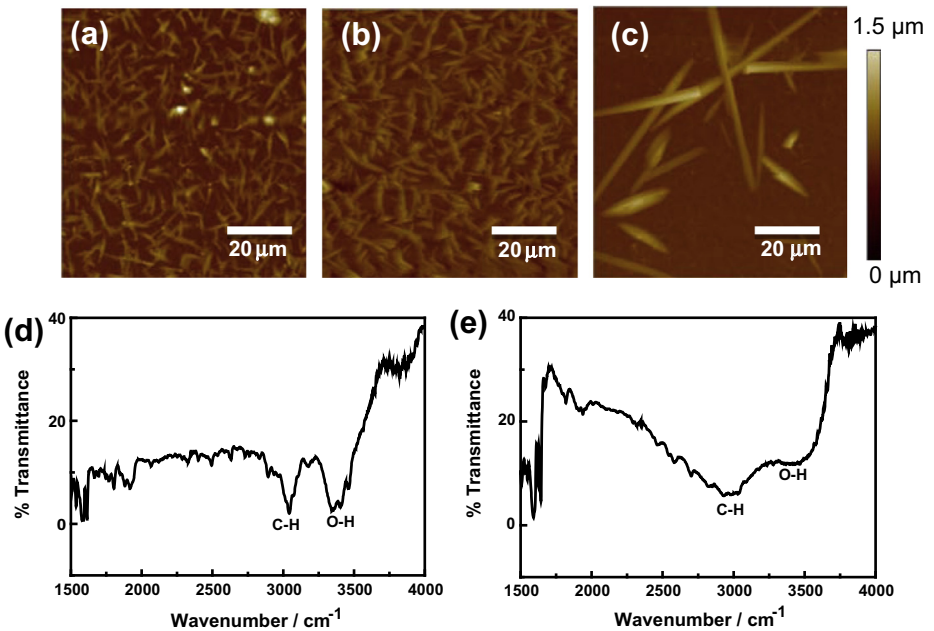

Fig. 4. (a–c) AFM images of pentacene/pyrene recorded in presence and absence of Cu^{2+}: (a) only Cu^{2+} ions; (b) both Cu^{2+} and Co^{2+} ions; (c) both Ba^{2+} and Co^{2+} ions; (d and e) FT-ATR spectra of the pyrene derivative in the (a) absence (only pyrene); (b) presence of Cu^{2+} ions.

Fig. S3 (ESI). Further study the self-assembly, we tried the reversible test, but the device remains irreversible because Cu^{2+} cannot be removed from the P–P* complexes in our drop-drying method.

3.4. CN^- ions sensitivity and selectivity studies in OTFTs

We also used our P-based device to monitor a set of anions (CN^-, PO_4^{3-}, I^-, HSO_4^-, F^-, NO^{3-}, ClO_4^-, Cl^-, Br^-). Among

these anions, the extremely toxic CN^- anion was the only one that provided a distinct change in the value of I_{sat}. Fig. 5 displays the performance of the device toward CN^- ions. In the presence of CN^- ions, the value of I_{sat} decreased by −1 μA, while the value of I_{off} was 1×10^{-8} A. But, F^- and Cl^- ions provided similar changes in the value of I_{off}, it was difficult to use this parameter alone to identify CN^- ions (Fig. S5 (ESI)). The differences in the values of I_{sat} arose mainly from the self-assembly of P in pentacene/P and the disappearance of the OH group to form a new benzoxazole ring upon adding the CN^- ions, as depicted in the insets to Fig. 5(a) and (b) [21]. In contrast the other testes ions (PO_4^{3-}, I^-, HSO_4^-, F^-, NO_3^-, ClO_4^-, Cl^-, Br^-) could not interact with the P ligands to form such benzoxazole rings, this device became a good sensor for CN^- ions. We elaborated the measurement to examine the analyses of pairs of anions in the presence (CN^-/F^- and CN^-/Br^-) and absence (HSO_4^-/F^- and $Cl^-/\{(PO_4^{3-}\})$ of CN^- ions (Fig. 5(c)). The data obtained for the pairs of ions were similar to those for the single ions; that is, the presence of CN^- ions decreased the value of I_{sat}, whereas it increased in its absence. Thus, our P-based device could be used for the detection of Cu^{2+} cations as well as CN^- anions. Because of their high toxicity, it is necessary for any sensor for CN^- ions to have nigh sensitivity; therefore, we tested our sensor for its ability to measure CN^- ions at concentrations ranging from 100 to 350 μM. Fig. 5(d) reveals that our pentacene/P transistor could detect CN^- ions at concentrations between 100 and 150 μM, with increased sensitivity upon increasing the concentration. To further test its potential applicability, we used our device to analyze sea water samples containing and free of CN^- ions, but we found that the performance was poor.

3.5. Sensing mechanisms of CN^- ions

To study the mechanism of the sensing of CN^- ions, we recorded AFM images (scale: 20×20 μm) and FT-ATR spectra. In the presence of CN^- ions (Fig. 6), the P rods broke into smaller pieces, as evidenced by the disappearance of the signal for the OH groups and the formation of fewer star-shaped assemblies. These star-shaped architectures did not arise from the coordination of the CN^- ions, but rather from the overlapping of two or three small P rods. To confirm this behavior, we recorded IR spectra of the sample in the presence of CN^- ions (Fig. 6(d)); the signal for the OH group at 3250–3500 cm^{-1} disappeared with broadening the aliphatic region near 3000 cm^{-1} and a new signal appeared at 2200 cm^{-1} for the benzoxazole units. Compared to pentacene the P with benzoxazole units were highly donating nature can accumulate more hole at the interface of pentacene and P (with benzoxazole). Since P with benzoxazole units spread all over the channel (Fig. 6(a)) which directly drop the I_{sat} by increasing the channel resistance. To confirm the mechanism, we prepared monolayer devices containing only pentacene and used anions (CN^-, F^-, Cl^-) to monitor the electrical behavior. In presence of these ions we observed only negligible changes in the device performance (see Fig. S6 (ESI)) and this conforms that the change in I_{sat} was only due to P

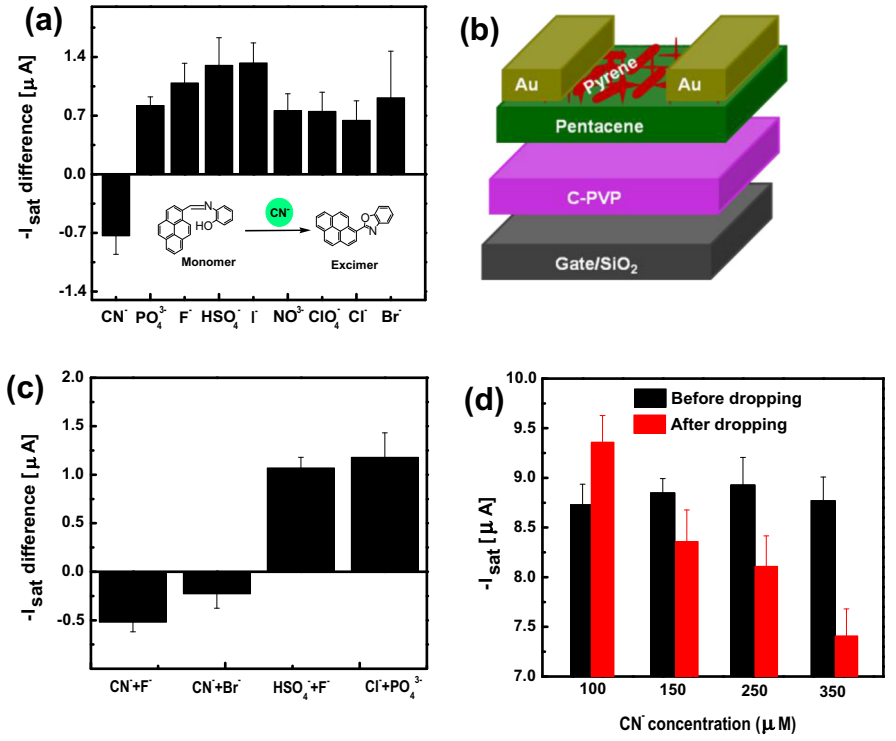

Fig. 5. (a) Changes in the value of I_{sat} in the presence of different anions. (b) Schematic representation of the self-assembly of the pyrene derivative in presence of CN^- ions. (c and d) Changes in the value of I_{sat} in the presence of (c) different pairs of mixed anions and (d) different concentrations of CN^- ions.

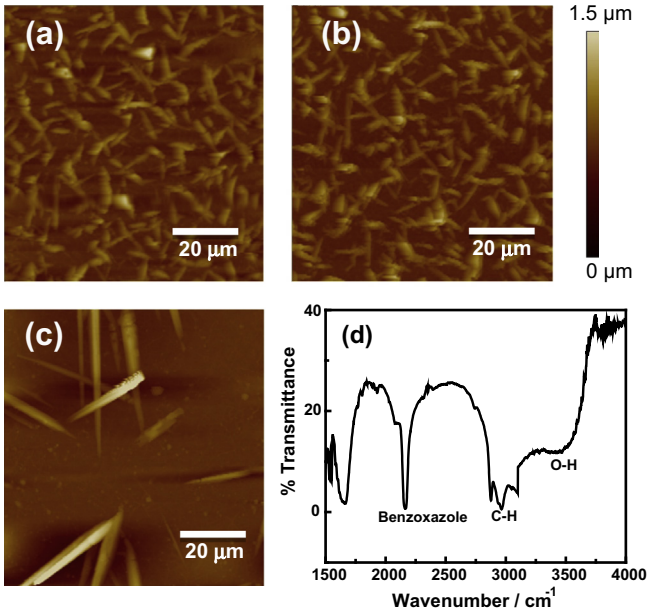

Fig. 6. (a–c) AFM images of pentacene/pyrene recorded in presence and absence of CN^-ions: (a) only CN^- ions; (b) both CN^- and F^- ions; (c) both HSO_4^- and F^- ions. (d) FT-ATR spectra of the pyrene derivative in the presence of CN^- ions.

(with benzoxazole) rods. Fig. 6(b) and (c) display the results obtained from studies extended to solutions of mixed ions. The AFM image of the sample prepared in the presence of mixed ions containing CN^- ions (Fig. 6(b)) was similar to that obtained for the sample prepared in the presence of CN^- ions alone; in the absence of CN^- ions, the image of the sample was unchanged. The change in the value of I_{sat}, but not in the values of V_{th} and I_{off}, was due only to the formation of the new benzoxazole ring. By comparing the performances of the pentacene-only devices with those of the pentacene/P devices, it was clear that the P units played a role in the detection of the Cu^{2+} and CN^- ions, but the cause of the changes in the values of I_{off} for the pentacene/P transistor in the presence of F^- and Cl^- ions remains unclear.

4. Conclusions

We have fabricated OTFTs based on pentacene/Schiff base pyrene derivative that can be used to detect both Cu^{2+} cations and highly toxic CN^- anions. For Cu^{2+} cations, the devices could be monitored sensitively through changes in the values of V_{th} and I_{off}; for CN^- anions, we monitored the value of I_{sat}. We found that Cu^{2+} ions could be detected at concentrations as low as 50 μM in both deionized water and sea water, but the CN^- ions could be detected only in deionized water in range from 100 to 150 μM. We confirmed the sensing mechanisms for both the Cu^{2+} and CN^- ions using AFM (scale: 20×20 μm) and FT-ATR spectroscopy. In the presence of both types of ions, the signal for the OH groups disappeared at 3250–3500 cm^{-1}; in the presence of Cu^{2+} ions, self-assembly to star-shaped rods occurred through P–P^* coordination, whereas in the presence of CN^- ions, the rods of the pyrene derivative broke into smaller pieces through the formation of benzoxazole rings, as evidenced by a new signal at 2200 cm^{-1}.

Acknowledgment

We thank the National Science Council of Taiwan (NSC 101-2221-E-001-010 and 101-2113-M-009-013-MY2) and Academia Sinica, Taiwan, for financial support.

Appendix A. Supplementary material

Supplementary data associated with this article can be found, in the online version, at http://dx.doi.org/10.1016/j.orgel.2013.12.007.

References

[1] (a) H. Yan, Z. Chen, Y. Zheng, C. Newman, J.R. Quinn, F. Dotz, M. Kastler, A. Facchetti, Nature 457 (2009) 679;
(b) A. Facchetti, Chem. Mater. 23 (2011) 733;
(c) Y. Wen, Y. Liu, Y. Guo, G. Yu, W. Hu, Chem. Rev. 111 (2011) 3358;
(d) P.M. Beaujuge, J.M.J. Fréchet, J. Am. Chem. Soc. 133 (2011) 20009.
[2] (a) P. Lin, F. Yan, Adv. Mater. 24 (2012) 34;
(b) M. Ramesh, H.-C. Lin, C.-W. Chu, J. Mater. Chem. 22 (2012) 16506;
(c) N. Liu, Y. Hu, J. Zhang, J. Cao, Y. Liu, J. Wang, Org. Electron. 13 (2012) 2781;
(d) H. Zhao, G. Dong, L. Duan, L. Wang, Y. Qiu, J. Phys. Chem. C 117 (2012) 58;
(e) Y. Peng, L. Lv, Y. Yao, F. Fan, C. Chen, Z. Zhou, W. Wang, G. Gao, Org. Electron. 14 (2013) 1045;
(f) S. Casalini, L. Leonardi, T. Cramer, F. Biscarini, Org. Electron. 14 (2013) 156.
[3] (a) L.W. Chang, Toxicology of Metals, Lewis Publishers, Boca Raton, FL, 1996;
(b) M.C. Linder, M. Hazegh-Azam, Am. J. Clin. Nutr. 63 (1996) 797S.
[4] E.S. Forzani, H. Zhang, W. Chen, N. Tao, Environ. Sci. Technol. 39 (2005) 1257.

[5] B. Vennesland, E.E. Comm, C.J. Knownles, J. Westly, F. Wissing, Cyanide in Biology, Academic Press, London, 1981.
[6] (a) K.W. Kulig, Cyanide Toxicity, U.S. Department of Health and Human Services, Atlanta, GA, 1991;
(b) Guidelines for drinking-water quality, World Health Organization: Geneva, (1996).
[7] (a) T.T. Christison, J.S. Rohrer, J. Chromatogr. A 31 (2007) 1155;
(b) K. Kaur, R. Saini, A. Kumar, V. Luxami, N. Kaur, P. Singh, S. Kumar, Coord. Chem. Rev. 256 (2012) 1992;
(c) G. Qian, X. Li, Z.Y. Wang, J. Mater. Chem. 19 (2009) 522.
[8] (a) L. Torsi, G.M. Farinola, F. Marinelli, M.C. Tanese, O.H. Omar, L. Valli, F. Babudri, F. Palmisano, P.G. Zambonin, F. Naso, Nat. Mater. 7 (2008) 412;
(b) F. Buth, A. Donner, M. Sachsenhauser, M. Stutzmann, J.A. Garrido, Adv. Mater. 24 (2012) 4511.
[9] M.L. Hammock, A.N. Sokolov, R.M. Stoltenberg, B.D. Naab, Z. Bao, ACS Nano 6 (2012) 3100.
[10] M. Ramesh, H.-C. Lin, C.-W. Chu, Biosens. Bioelectron. 42 (2013) 76.
[11] (a) H.L. Cheng, Y.S. Mai, W.Y. Chou, L.R. Chang, X.W. Liang, Adv. Funct. Mater. 17 (2007) 3639;
(b) H. Dong, C. Wang, W. Hu, Chem. Commun. 46 (2010) 5211;
(c) M.E. Roberts, N. Queraltó, S.-C.B. Mannsfeld, B.-N Reinecke, W. Knoll, Z. Bao, Chem. Mater. 21 (2009) 2292.
[12] (a) S. Karuppannan, J.-C. Chambron, Chem. Asian J. 6 (2011) 964;
(b) R. Martínez-Máñez, F. Sancenón, Chem. Rev. 103 (2003) 4419.
[13] (a) M.A. Cejas, F.M. Raymo, Langmuir 21 (2005) 5795;
(b) R. Stine, S-P. Mulvaney, J-T. Robinson, R. Tamanaha, P.-E. Sheehan, Anal. Chem. 85 (2013) 509.
[14] (a) M.E. Østergaard, P.J. Hrdlicka, Chem. Soc. Rev. 40 (2011) 5771;
(b) Y. Yubin, S. Ji, F. Zhou, J. Zhao, Biosens. Bioelectron. 24 (2009) 3442.
[15] (a) J. Kwon, J.-P. Hong, S. Noh, T.-M. Kim, J-J. Kim, C. Lee, S. Lee, J.-I. Hong, New J. Chem. 36 (2012) 1813;
(b) T.-M. Figueira-Duarte, K. Müllen, Chem. Rev. 111 (2011) 7260.
[16] (b) K. Takemoto, M. Karasawa, M. Kimura, ACS Appl. Mater. Interface 4 (2012) 6289;
(c) C.-C. Yu, K.-J. Jiang, J.-H. Huang, F. Zhang, F.-W. Wang, L.-M. Yang, Y. Song, X. Bao, Org. Electron. 14 (2013) 445;
(d) J.-W. Mun, I. Cho, D. Lee, W.S. Yoon, O.K. Kwon, C. Lee, S.Y. Park, Org. Electron. 14 (2013) 2341.
[17] (a) L. Basabe-Desmonts, D.N. Reinhoudt, M. Crego-Calama, Chem. Soc. Rev. 36 (2007) 993;
(b) J.-M. Kim, S.J. Min, S.W. Lee, J.H. Bok, J.S. Kim, Chem. Commun. (2005) 3427.
[18] M. Shellaiah, Y.-H. Wu, A. Singh, M.V. Ramakrishnam Raju, H.-C. Lin, J. Mater. Chem. A 1 (2013) 1310.
[19] H. Klauk, M. Halik, U. Zschieschang, G. Schmid, W. Radlik, W. Weber, J. Appl. Phys. 92 (2002) 5259.
[20] R.L. Prasad, A. Kushwaha, O.N. Shrivastava, J. Solid State Chem. 196 (2012) 471.
[21] L. Zang, D. Wei, S. Wang, S. Jiang, Tetrahedron 63 (2012) 636.